Investigation of Ultrasound-Measured Flow Rate and Wall Shear Rate in Wrist Arteries Using Flow Phantoms

Zhou, Xiaowei; Xia, Chunming; Khan, Faisel; Corner, George A.; Huang, Zhihong; Hoskins, Peter R.

Published in:
Ultrasound in Medicine and Biology

DOI:
10.1016/j.ultrasmedbio.2015.10.016

Publication date:
2016

TECHNICAL NOTE: INVESTIGATION OF ULTRASOUND-MEASURED FLOW RATE AND WALL SHEAR RATE IN WRIST ARTERIES USING FLOW PHANTOMS

XIAOWEI ZHOU*, CHUNMING XIA‡, FAISEL KHAN§, GEORGE A CORNER*, ZHIHONG HUANG*, and PETER R HOSKINS†

*School of Engineering, Physics & Mathematics, University of Dundee, Dundee, United Kingdom

† Centre for Cardiovascular Science, University of Edinburgh, Edinburgh, United Kingdom

§ Cardiovascular and Diabetes Medicine, Ninewells Hospital and Medical School, University of Dundee, Dundee, United Kingdom

‡ School of Mechanical and Power Engineering, East China University of Science and Technology, Shanghai, China

Short title: investigation of flow rate and wall shear rate with ultrasound

Address correspondence to: Zhihong Huang, School of Engineering, Physics & Mathematics, Fulton Building, Dundee, DD1 4HN, UK. Tel: +441382385477. E-mail: z.y.huang@dundee.ac.uk

Abstract- The aim of this study is to evaluate the errors in measurement of volumetric flow rate and wall shear rate measured in radial and ulnar arteries using a commercial ultrasound scanning system. The Womersley equations are used to estimate the flow rate and wall shear rate waveforms, based on the measured vessel diameter and centreline velocity waveform. In the experiments, each variable (vessel depth, diameter, flow rate, beam-vessel angle and different waveform) in the phantom is investigated in turn and its value varied within a normal range while others were fixed at their typical values. The outcomes show flow rate and wall shear rate are overestimated in all cases, from around 13% up to nearly 50%. It is concluded that measurements of flow rate and wall shear rate in radial and ulnar arteries with clinical ultrasound scanner are prone to overestimation.

Key Words: **Radial artery, Ulnar artery, Flow rate, Wall shear rate, Womersley, Doppler ultrasound, Flow phantoms.**

INTRODUCTION

In the last decade, the number of cases investigating the blood flow in radial and ulnar arteries using ultrasound imaging has grown. One of the common instances is the catheterization of the coronary arteries. Before the catheterization, ultrasound imaging is often used to obtain the blood flow rate in ulnar artery to make sure that the collateral circulation via the ulnar artery is adequate to perfuse the hand (Habib et al. 2012). Measuring the volumetric flow rate and resistive index of flow waveform in the ulnar artery is also a requirement in cannulation of the radial artery and radial harvesting for coronary surgery (Gaudino et al. 2005; Royse et al. 2008; Kim et al. 2012). The blood flow velocities and waveforms in radial and ulnar arteries have been used to evaluate sympathetic skin response between healthy subjects and patients after stroke (Tiftik et al. 2014). Flow rates measured with ultrasound in the radial and ulnar arteries can also be used to distinguish different forms of Raynaud's diseases that are caused by lack of blood supply from radial and ulnar arteries to fingers (Toprak et al. 2009; Toprak et al. 2011).

The methods used for estimating the flow rate in these studies estimates the flow rate simply through the product of maximum velocity and blood vessel area (Ozcan et al. 2011; Toprak et al. 2011; Tiftik et al. 2014). Further, no consideration in the literature has been given to evaluate the accuracy or reliability of these measurements. Measurements of flow rate in arteries with ultrasound imaging are prone to errors (Li et al. 1993; Steinman et al. 2001; Swillens et al. 2009; Ponzini 2010). The validation for flow rates in arteries has been implemented by researchers using an experimental system referred to as "phantom" (Leguy et al. 2009; Hoskins et al. 2010; Ricci et al. 2013). A review of validation of arterial ultrasound imaging and blood flow was also provided by Hoskins(2008). These studies mostly consider measurement of flow rate in larger arteries such as the carotid and femoral which have diameters in the range 5-10 mm. The radial and ulnar arteries have a smaller diameter of 2-3 mm (Habib et al. 2012) and have a lower flow rate of 50 ml min^{-1} (Manabe et al. 2005). There has been no specific investigation of the errors in flow rate relevant to the ulnar and radial arteries.

In addition to flow rate, one other parameter which will be investigated in this study is wall shear rate. The wall shear rate, which is relevant to wall shear stress being sensed through sensors within the endothelium and thought to be part of a control mechanism in the arterial wall(Davies 1995), has been attracting great interest over years (Hoeks et al. 1995; Blake et al. 2008; Mynard et al. 2013). Obtaining the wall shear rate values in radial and ulnar arteries should provide more clinical information for diseases related to these two arteries. However, there has been no study measuring wall shear rate in radial and ulnar arteries and evaluating their errors.

The aim of this study is to evaluate these errors of volumetric flow rate (FR) and wall shear rate (WSR), based on ultrasound measurements made in a flow phantom.

METHODS

Overview

A method developed by Blake et al. (2008) was used to estimate volumetric flow rate and wall shear rate simultaneously. This relies on measurement of the maximum Doppler frequency from spectral Doppler and diameter from the B-mode image which can be obtained from the digital image data without the need for RF or IQ data. These are used as input to the Womersley equations. The output is the time-varying velocity profile from which the volumetric flow waveform and the wall shear rate waveform are calculated. It is noted that the method assumes fully-developed flow.

Theory

Womersley equations were used to derive the time-varying velocity profile of the pulsatile flow in a long, rigid wall pipe (Womersley 1955). The original Womersley equations estimate velocity profiles with input of the mean velocity – time waveform. Holdsworth (1999) modified the Wonersley equations so that the centre-line velocity could be input instead of the mean velocity. The centre line velocity corresponds to the maximum velocity, apart from a brief period where the

flow is changing direction. This formulation then allows the maximum velocity – time waveform obtained from spectral Doppler to be used as input to the Womersley equations. This method was used by Blake et al. (2008) for estimation of wall shear rate, and this study follows the same methodology. Vessel diameter is measured using B-mode imaging. The velocity profile $v_f(y,t)$ in arteries can be calculated:

$$v_f(y,t) = \sum_{k=0}^{+\infty} \mathrm{Re}\left\{ V_k e^{j(k\omega t - \varphi_k)} \left[\frac{J_0(\tau_k) - J_0(\tau_k y)}{J_0(\tau_k) - 1} \right] \right\} \quad (1)$$

where *Re* represents the real part of a complex function; J_0 is the zero order Bessel functions of the first kind. y is the normalised radial coordinate; ω is the angular frequency; t is time; φ_k represents the phase of each harmonic; V_k is the centreline velocity of each harmonic; and τ_k is represented by $\alpha_k * j^{3/2}$. α_k is the Womersley number for each harmonic,

$$\alpha_k = R\sqrt{\frac{k\omega}{\nu}} \quad (2)$$

Where ν is the kinematic viscosity of the fluid and R is the diameter. After obtaining the time-varying velocity profile, the flow rate $Q(t)$ can be derived using equation 3:

$$Q(t) = 2\pi \int_0^R v_f(y,t) y \partial y \quad (3)$$

Wall shear rate $wsr(t)$, is calculated using equation 4:

$$wsr(t) = \left. \frac{\partial v_f(y,t)}{\partial y} \right|_{y=R} \quad (4)$$

Figure 1 gives the schematic of estimating flow rate and wall shear rate using the Womersley equations method.

Flow phantom

The flow phantoms were made with acoustically equivalent tissue-mimicking materials (Fig. 1). A straight blood vessel mimic made from polyvinyl alcohol cryogel (PVA-c) subject to 6 freeze-thaw cycles (Dineley et al. 2006) was embedded at a known depth within the agar-based tissue

mimic (Teirlinck et al. 1998). The PVA-c vessel set in a Perspex box was filled with water and sealed at both ends to generate a resistance while pouring the tissue mimic. A blood mimic based on nylon particles was used with acoustic properties and viscosity matched to blood (Ramnarine et al. 1998).

Pulsatile flow patterns were achieved through connecting a gear pump (Micropump® Series GA-X21, Vancouver, WA, USA) to the inflow of the phantom loop. The pump was controlled by Labview 2010 (National Instruments, Austin, TX, USA) to generate different flow waveforms in the blood vessel.

The depth of the blood vessel was chosen in the range of 5 to 6 mm. The thickness of the vessel wall was 2 mm. For each assembled phantom 9% glycerol was added on the top of agar-based tissue mimic in the Perspex box to provide ultrasound coupling. The depth at which the vessel was positioned within the ultrasound image could be varied by adjusting the position of the transducer relative to the vessel through the use of a scanning well filled with speed-of-sound corrected water-glycerol solution. Four flow phantoms were made having different vessel diameters, and labelled as phantom 1 to 4.

The true average flow rate in volume was measured using timed-collection with a measuring cylinder and stopwatch. The true average wall shear rate was estimated using equation 5 (Hoskins 2011):

$$\frac{dv}{dr} = \frac{8v_{mean}}{D} \qquad (5)$$

where v_{mean} is the flow rate, D represents diameter of the vessel.

Use of the Womersley equations assumes fully developed flow. The inlet length was estimated using equation 6 with values of 3.3mm^2 s^{-1} for viscosity (Ramnarine et al. 1998), 4 mm for diameter and 1.33 m s^{-1} for mean velocity when volumetric flow rate is at maximum of 100ml min^{-1}. The inlet length was 26 mm confirming that the ultrasound data was acquired in a region of fully developed flow.

$$L = 0.04\frac{v_{mean}d^2}{v} \quad (6)$$

Experimental protocol

Blood vessel depths, beam-vessel angles, flow rates, vessel diameters and flow waveforms were investigated to evaluate their effects on the flow rate and wall shear rate estimations. The ranges of these variables were based on published data and a preliminary set of measurements which were made on 15 normal volunteers to help inform the choice of diameter, depth, flow rate and waveform, and are shown in table 1 and fig. 2.

Spectral velocity waveforms from the radial or ulnar artery were quite different among the 15 volunteers. Therefore, an averaged waveform from 15 volunteers' spectral Doppler velocity outlines in both radial and ulnar arteries was adopted as the typical centreline velocity waveform in the experiment, which was indicated in waveform 1 in fig. 2.

The flow mediated method has been often used to study the artery-relevant diseases in the arm (Agewall et al. 2001; Moens et al. 2005; Stout 2009). In the flow mediated method, the brachial artery was blocked for five minutes with a pressure cuff. The dynamics of the downstream flow is then studied from the moment when the cuff is released. Waveforms in this case will be quite non-typical. To allow fully consideration of different waveforms of radial and ulnar arteries in clinical research and clinical practice, waveforms from different stages of flow mediated experiment in a healthy volunteer were also used in this study, as shown in waveform 2, 3 and 4 in figure 3. Volunteers were told not to consume any food other than water within 2 hours before the experiment and asked to take a rest at least five minutes to allow them to relax. The room temperature was about 22 ±1ºC. The experimental protocol for these measurements was reviewed and approved by the Research Ethics Committee of Dundee University and all volunteers gave their written informed consent to participate.

The typical value for each variable was chosen. This was 10mm for vessel depth, 68° for beam-vessel angle, 2.60 mm for the diameter, 40 ml min^{-1} for the flow rate and the waveform 1

(Fig. 2) for the waveform. In the experiments, only one variable was altered at a time in turn while the others were set at their typical value.

Ultrasound data acquisition and processing

Data acquisition. A Philips HDI 5000 clinical ultrasound scanner was used to collect all the data from the flow phantom and volunteers. A L12-5 transducer with B-mode frequency10 MHz and Doppler frequency 6 MHz was used. The diameters from each frame of the B-mode were averaged through several cardiac cycles. The centreline velocity in the vessel was obtained from the spectral Doppler mode with the sample volume placed centrally in the vessel. In order to achieve the accurate measurements both for diameter and centreline velocity, the transducer was adjusted to get the clearest view of the vessel and the sonogram in the longitudinal orientation (Fig. 3). The wall filter was set to low and Doppler gain was adjusted to give spectral Doppler traces with consistent brightness for all measurements. The sample gate size was 2.0 mm which is enough to cover the centreline of the vessel to get maximum velocity. The measurements were repeated six times with the transducer repositioned between each.

Data processing. The data obtained from the ultrasound machine was processed in MATLAB R2013b (The MathWorks, Natick, MA, USA). An in-house developed MATLAB code was used to read the binary files generated from the cine loop memory of the ultrasound scanner. The diameter of the blood vessel within the phantom was measured using the distance-intensity method (Blake et al. 2008). The distance-intensity method uses the intensity differences of the reflected B-mode signal between lumen and tissue to estimate the vessel diameter. As shown in fig. 5, each frame of B-mode images was used to obtain vessel diameter at the pixel level by searching the peak points on the distance-intensity curve resulting from the strong reflection from both inner surfaces of blood vessel. The diameter was obtained by averaging time-varying diameter waveform over integers of cardiac cycle.

For the centreline velocity, over 10 cycles of the peak velocity waveform in Doppler ultrasound's sonogram were averaged into one single cycle. The averaged diameter and one cycle of velocity waveform were processed as indicated in fig 1 to calculate flow rate and wall shear rate waveforms over one cardiac cycle. Finally the time-averaged flow rate and wall shear rate were calculated from their waveforms. With the estimated time-averaged flow rate and wall shear rate (repeated six times under each circumstance), the percentage error in form of mean ± standard deviation was calculated based on the true average flow rate from timed-collection and true average wall shear rate from equation 5.

RESULTS

Diameter measurement

Figure 5 shows the diameter waveform of the blood vessel in phantom 2 over two cardiac cycles when the flow rate is 40 ml min^{-1}. The vessel diameter in the phantom is not constant. It changes with the pulsatile flow in the vessel.

Table 2 lists the diameters of phantom 1 to 4, measured in both static and pulsatile conditions. The diameters of blood vessel in phantom 1 to phantom 4 under static condition were at 1.86(0.02) mm, 2.60(0.03) mm, 2.89(0.03) mm and 3.49(0.04) mm. The mean diameter of vessel in the pulsatile condition was greater than the diameter in static condition.

Flow rate and wall shear rate from Womersely equations

The Womersley equations method could estimate the time-varying waveforms of flow rate and wall shear rate over the cardiac cycle in the flow phantom.

Figure 7 to Figure 11 show the error estimations of flow rate and wall shear rate with different vessel depths, beam-vessel angles, flow rates, vessel diameters and flow waveforms. From these figures, it can be seen that all results, both for flow rate and for wall shear rate, are

overestimated in a range of 13% to nearly 50%. In fig. 7, 9, 11, with different vessel depths, flow rates and flow waveforms, the overestimation errors remains at the same level, indicating that different vessel depths, flow rates and waveforms do not have an obvious effect on flow rate and wall shear rate estimations.

However, vessel diameter and beam-angle do effect the flow rate and wall shear rate estimations. When the beam-vessel angle increased from 38° to 68° (Fig. 8), the overestimation shifted from around 14% to 35%. The overestimation was only about 13% for vessel diameter at 1.86mm, but around 35% at 2.60 mm and 2.89 mm, going up dramatically to nearly 50% at the vessel diameter of 3.49 mm (Fig. 10).

DISCUSSION

This study used PVA-c blood vessel mimic coupled with agar-based tissue mimic in the phantoms. It was found that the vessel was slightly compressed into an ellipse-like shape within transverse plane due to a pressure generated by weight of the tissue mimic above the vessel. The non-circular vessel may lead to the underestimation of the vessel diameter, and may also have an effect on the estimation of velocity profile based on Womersley. Despite measures taken to minimise the non-circularity effect, including burying the vessel at only a shallow depth within tissue mimic, making the PVA-vessel wall thicker and filling the vessel with water while pouring the tissue mimic, a difference between the horizontal and vertical directions (less than 0.1 mm) within the cross-sectional plane of the vessel still existed. The non- circularity may have some effects on the estimations of flow rate and wall shear rate.

The error in flow rate and wall shear rate ranged from 14% to 35%, depending on beam-vessel angle from 38° to 68°. The flow rate and wall shear rate were derived based on the maximum velocity measured from Doppler ultrasound. The estimation errors in flow rate and wall shear rate in this study were consistent with the previously reported estimation error caused by the geometric

spectral broadening in maximum velocity (Hoskins 1996; Hoskins 1999; Steinman et al. 2001). Therefore, the angle-dependent maximum velocity estimation led to the corresponding errors in flow rate and wall shear rate estimations. In this study, 68° was chosen as the typical beam-vessel angle, because, in most cases, the angle was near 68° when placing the linear array transducer on the surface of the human wrist to which the radial and ulnar arteries are parallel. As a result, the flow rate and wall shear rate were obviously overestimated when studying all other variables, shown in fig. 7, 9, 10 and 11. As proposed in many published studies, angle corrections can be conducted to reduce the inaccuracies in estimating the maximum velocity due to angle-dependence (Hoskins 1996; Hoskins 2008), which consequently should reduce the inaccuracies of estimation in flow rate and wall shear rate.

Errors in measurements of vessel diameter have a crucial effects on the estimate of flow rate and wall shear rate (Hoskins et al. 2010; Vergara et al. 2010a). In this study, accurate measurement of the vessel diameters is very important in three areas in particular. The Womersley equations for deriving the velocity profile (shown in equation 1) is sensitive to the measurements of vessel diameter (Vergara et al. 2010b). As indicated in equation 3 and 4, the calculations of flow rate and wall shear rate are determined by the measurement of vessel diameter. Further, the mean wall shear rate calculated by equation 5 is based on the estimated vessel diameter. However, for this work there was no knowledge as to the true diameters of the vessels after fabrication of the phantom. In clinical practice, visualizing the radial and ulnar arteries with ultrasound will not be as easy as on the flow phantom. A high frequency transducer is necessary to measure the diameter accurately. Since the depth of the radial and ulnar arteries is small, attenuation in using a high frequency transducer will not be a problem in clinical practice.

The overestimation was less at flow rates above 40 ml min^{-1}. This is explained by the average diameter of the blood vessel being underestimated at high flow rates. Higher flow rates going through the tube could increase the amplitude of vessel wall motion, leading to a higher velocity of blood vessel wall in radial direction. Therefore, if the B-mode frame rate was too low, it

may not be fast enough to capture the fast motion of the vessel wall, causing the underestimation of the diameter. Frame rates of 17 fps and 34 fps in B-mode were both used to measure the diameter during the study. We also found that the estimated diameters of vessel at the flow rate over 40 ml min^{-1} with 17 fps were smaller than the diameters measured with 34 fps. However, 34 fps was the upper limit frame rate at this depth for the HDI5000 scanner and may not be enough to capture the fast-moving vessel motion. According to equation 3 and equation 5, the underestimation of vessel diameter could reduce overestimation (compared to flow rate no more than 40 ml min^{-1}) of flow rate and wall shear rate. A higher frame rate should be used to capture the fast motion when measuring vessel diameter in B-mode if possible.

Although a high flow rate up to 100 ml min-1 was applied within the vessel made of PVA-c shown in Table 2, the vessel diameter could return to its original size 2.60 ± 0.03 mm once the flow rate reduced. The greatest extension of the PVA-c was comfortably less than 30% in the radial direction (about 25%, from 2.60 mm to 3.25 mm).

When the flow rate was kept at 40 ml min^{-1} (fig. 10), the overestimation increased as the diameter of the vessel changed from 1.86 mm to 3.49 mm. This increase in overestimation may be attributed to the larger error in measurement of larger vessel diameter but another possibility is that the vessel diameter had an effect on the estimation of flow rate and wall shear rate when the true flow rate in the flow loop was kept at the same level.

It was found the waveforms did not influence the measurement. However only single flow direction in the phantom was investigated and there was no reverse flow. The fact is that the reverse flow was found in the radial and ulnar arteries of very few volunteers. The reverse flow pattern may have an effect on the Womersley-based calculations.

The same velocity profile calculated by inputting diameter and centreline velocity into Womersley equations was used to derive both flow rate and wall shear rate. The references for mean flow rate and mean wall shear rate in the phantoms were estimated based on time collected and Hagen–Poiseuille approach respectively. Although the references were different and unrelated,

the percentage errors of flow rate and wall shear rate were consistent, which suggests that the derived velocity profile based on Womersley equations was reliable.

This study is the first one to validate the measurements of volumetric flow rate and wall shear rate in radial and ulnar arteries using a clinical ultrasound scanner with the flow phantoms. This Womersley equations method can be readily applied in clinical practice providing the scanner can provide spectral Doppler and B-mode image data(Yang et al. 2013).

CONCLUSION

In this study, the measurement and validation of flow rate and wall shear rate in radial and ulnar arteries are described based on the soundly-designed flow phantoms which mimicked these two arteries in depth, diameter, flow rate, flow waveform and also the beam-vessel angle when using the ultrasound imaging technologies. Generally, the flow rate and wall shear rate were both overestimated from around 13% to 50%. Beam-vessel angle and vessel diameter appeared to affect the estimations while vessel depth, flow rate and flow waveform did not. Overestimations of flow rate and wall shear rate may be caused by the overestimation of maximum velocity when using spectral Doppler ultrasound. In clinical practice, these overestimations can lead to misunderstandings when it comes to diagnosing the diseases which are relevant to the flow rate and wall shear rate in radial and ulnar arteries.

ACKNOWLEDGEMENTS

The authors gratefully acknowledge Dr David Kenwright and Dr Efstratios Kokkalis for their great assistance of making the flow phantom. This work is supported by China Scholarship Council (CSC) and University of Dundee.

REFERENCES

Agewall S, Doughty RN, Bagg W, G.A.Whalley, G.Braatvedt, N.Sharpe. Comparison of ultrasound assessment of flow-mediated dilatation in the radial and brachial artery with upper andforearm cuff positions. Clin Physiol 2001;21:9-11.

Blake JR, Meagher S, Fraser KH, Easson WJ, Hoskins PR. A method to estimate wall shear rate with a clinical ultrasound scanner. Ultrasound in Medicine & Biology 2008;34:760-74.

Davies PF. Flow-mediated endothelial mechanotransduction. Physiol Rev 1995;75:519-60.

Dineley J, Meagher S, Poepping TL, McDicken WN, Hoskins PR. Design and characterisation of a wall motion phantom. Ultrasound in Medicine & Biology 2006;32:1349-57.

Gaudino M, Serricchio M, Tondi P, Gerardino L, Di Giorgio A, Pola P, Possati G. Chronic compensatory increase in ulnar flow and accelerated atherosclerosis after radial artery removal for coronary artery bypass. J Thorac Cardiovasc Surg 2005;130:9-12.

Habib J, Baetz L, Satiani B. Assessment of collateral circulation to the hand prior to radial artery harvest. Vasc Med 2012;17:352-61.

Hoeks APG, Samijo SK, Brands PJ, Reneman RS. Noninvasive Determination of Shear-Rate Distribution across the Arterial Lumen. Hypertension 1995;26:26-33.

Hoskins PR. Accuracy of maximum velocity estimates made using Doppler ultrasound systems. Brit J Radiol 1996;69:172-7.

Hoskins PR. A comparison of single- and dual-beam methods for maximum velocity estimation. Ultrasound Med Biol 1999;25:583-92.

Hoskins PR. Simulation and Validation of Arterial Ultrasound Imaging and Blood Flow. Ultrasound in Medicine & Biology 2008;34:693-717.

Hoskins PR. Estimation of blood velocity, volumetric flow and wall shear rate using Doppler ultrasound. Ultrasound 2011;19:120-9.

Hoskins PR, Soldan M, Fortune S, Inglis S, Anderson T, Plevris J. Validation of Endoscopic Ultrasound Measured Flow Rate in the Azygos Vein Using a Flow Phantom. Ultrasound Med Biol 2010;36:1957-64.

Kim SY, Lee JS, Kim WO, Sun JM, Kwon MK, Kil HK. Evaluation of radial and ulnar blood flow after radial artery cannulation with 20-and 22-gauge cannulae using duplex Doppler ultrasound. Anaesthesia 2012;67:1138-45.

Leguy CA, Bosboom EM, Hoeks AP, van de Vosse FN. Model-based assessment of dynamic arterial blood volume flow from ultrasound measurements. Med Biol Eng Comput 2009;47:641-8.

Li S, Mcdicken WN, Hoskins PR. Blood-Vessel Diameter Measurement by Ultrasound. Physiol Meas 1993;14:291-7.

Manabe S, Tabuchi N, Tanaka H, Arai H, Sunamori M. Hand circulation after radial artery harvest for coronary artery bypass grafting. J Med Dent Sci 2005;52:101-7.

Moens AL, Goovaerts I, Claeys MJ, Vrints CJ. Flow-mediated vasodilation: A diagnostic instrument, or an experimental tool? Chest 2005;127:2254-63.

Mynard JP, Wasserman BA, Steinman DA. Errors in the estimation of wall shear stress by maximum Doppler velocity. Atherosclerosis 2013;227:259-66.

Ozcan HN, Kara M, Ozcan F, Bostanoglu S, Karademir MA, Erkin G, Ozcakar L. Dynamic Doppler evaluation of the radial and ulnar arteries in patients with carpal tunnel syndrome. AJR Am J Roentgenol 2011;197:W817-20.

Ponzini R. Womersley Number-Based Estimates of Blood Flow Rate in Doppler Analysis In Vivo Validation by Means of Phase-Contrast MRI. 2010;

Ramnarine KV, Nassiri DK, Hoskins PR, Lubbers J. Validation of a new blood-mimicking fluid for use in Doppler flow test objects. Ultrasound Med Biol 1998;24:451-9.

Ricci S, Cinthio M, Ahlgren AR, Tortoli P. Accuracy and reproducibility of a novel dynamic volume flow measurement method. Ultrasound in Medicine & Biology 2013;39:1903-14.

Royse AG, Chang GS, Nicholas DM, Royse CF. No late ulnar artery atheroma after radial artery harvest for coronary artery bypass surgery. Ann Thorac Surg 2008;85:891-5.

Steinman AH, Tavakkoli J, Myers JG, Cobbold RSC, Johnston KW. Sources of error in maximum velocity estimation using linear phased-array Doppler systems with steady flow. Ultrasound Med Biol 2001;27:655-64.

Stout M. Flow-mediated dilatation: a review of techniques and applications. Echocardiography 2009;26:832-41.

Swillens A, Lovstakken L, Kips J, Torp H, Segers P. Ultrasound Simulation of Complex Flow Velocity Fields Based on Computational Fluid Dynamics. Ieee T Ultrason Ferr 2009;56:546-56.

Teirlinck CJPM, Bezemer RA, Kollmann C, Lubbers J, Hoskins PR, Fish P, Fredfeldt KE, Schaarschmidt UG. Development of an example flow test object and comparison of five of these test objects, constructed in various laboratories. Ultrasonics 1998;36:653-60.

Tiftik T, Kara M, Ozcan HN, Turkkan C, Ural FG, Ekiz T, Akkus S, Ozcakar L. Doppler ultrasonographic evaluation of the radial and ulnar arteries in hemiparetic patients after stroke. J Clin Ultrasound 2014;

Toprak U, Hayretci M, Erhuner Z, Tascilar K, Ates A, Karaaslan Y, Karademir MA. Dynamic Doppler Evaluation of the Hand Arteries to Distinguish Between Primary and Secondary Raynaud Phenomenon. Am J Roentgenol 2011;197:W175-W80.

Toprak U, Selvi NA, Ates A, Erhuner Z, Bostanoglu S, Karademir MA, Karaaslan Y. Dynamic Doppler evaluation of the hand arteries of the patients with Raynaud's disease. Clin Rheumatol 2009;28:679-83.

Vergara C, Ponzini R, Veneziani A, Redaelli A, Neglia D, Parodi O. Womersley number-based estimation of flow rate with Doppler ultrasound: sensitivity analysis and first clinical application. Comput Methods Programs Biomed 2010a;98:151-60.

Vergara C, Ponzini R, Veneziani A, Redaelli A, Neglia D, Parodi O. Womersley number-based estimation of flow rate with Doppler ultrasound: sensitivity analysis and first clinical application. Comput Methods Programs Biomed 2010b;98:151-60.

Womersley JR. Method for the Calculation of Velocity, Rate of Flow and Viscous Drag in Arteries When the Pressure Gradient Is Known. J Physiol-London 1955;127:553-63.

Yang X, Hollis L, Adams F, Khan F, Hoskins PR. A fast method to estimate the wall shear stress waveform in arteries. Ultrasound 2013;21:23-8.

Figures.

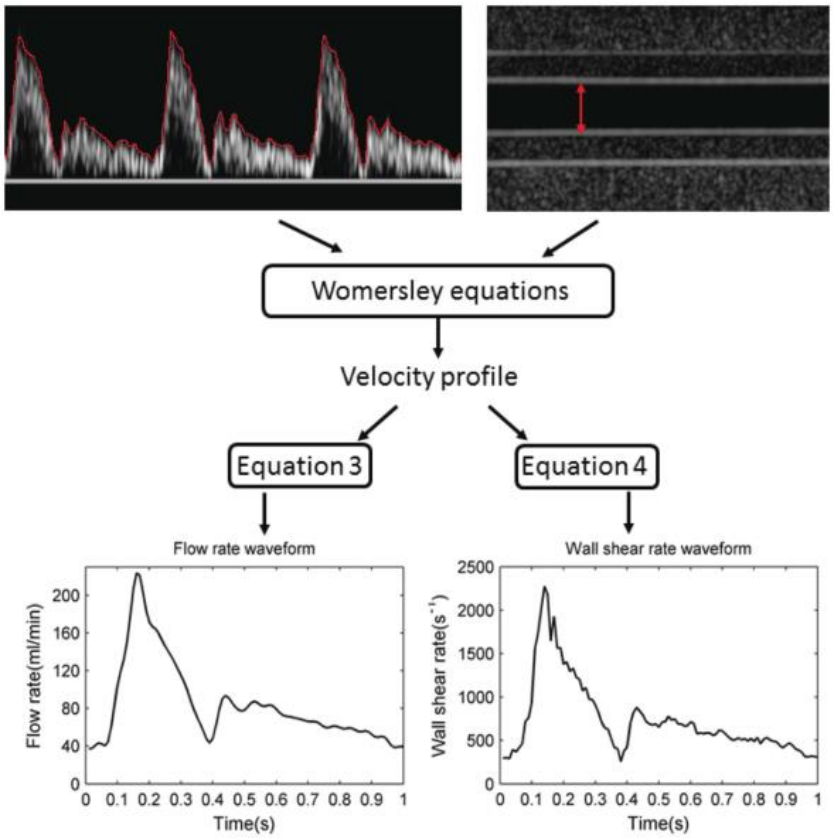

Fig. 1. Estimation of volumetric flow and wall shear rate wavefroms using the Womersley equations method. The maximum velocity waveform and the diameter are used in Womersley equations. The resulted velocity profile is then used to calcuate the volumetric flow and wall shear rate waveforms. The schematic shown is from the phantom where the flow rate is 40ml min^{-1} and the diameter is 2.89mm.

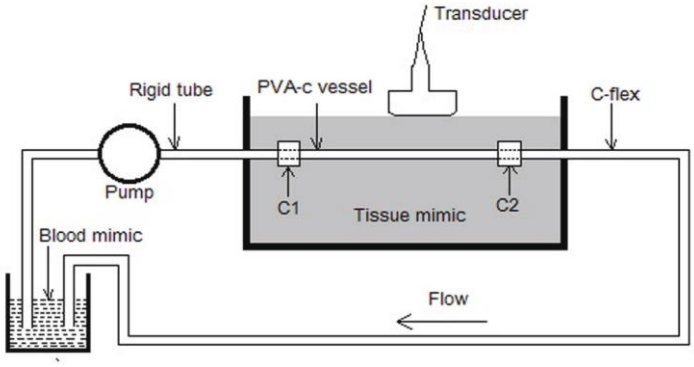

Fig. 2. The diagram of flow phantom

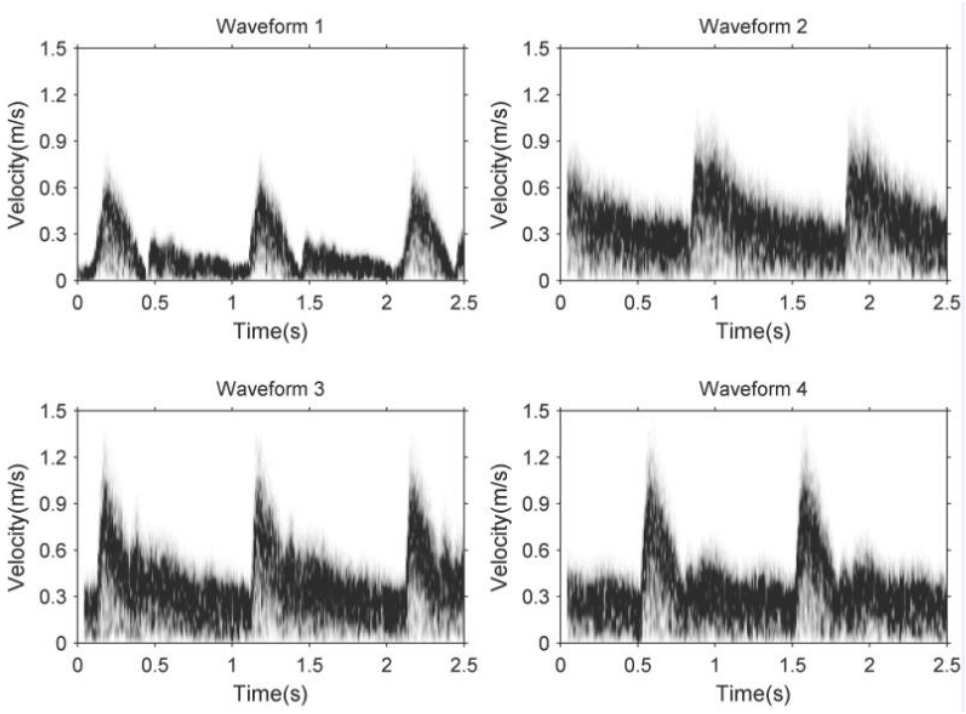

Fig. 3. Four different waveforms used in the flow phantom

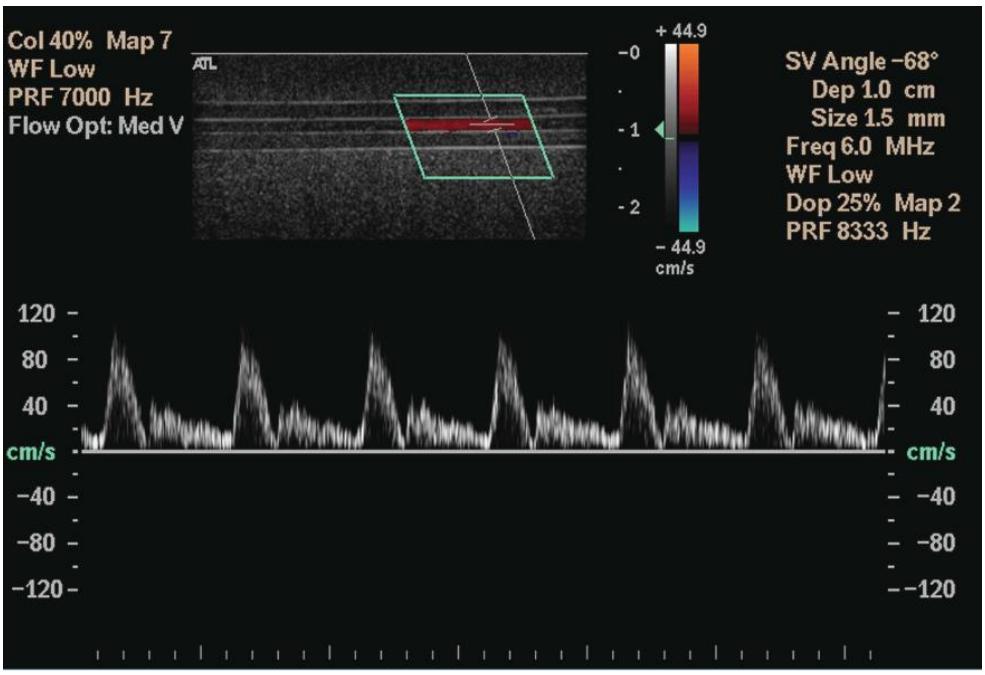

Fig. 4. The data collecting image with ultrasound scanner

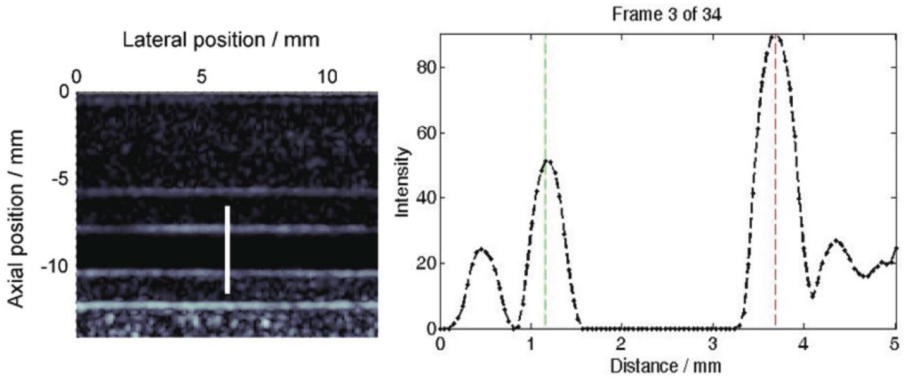

Fig. 5. The distance-intensity method to measure the diameter of the vessel, the white line on the left picture indicating measurement position and the right picture giving the corresponding distance-intensity.

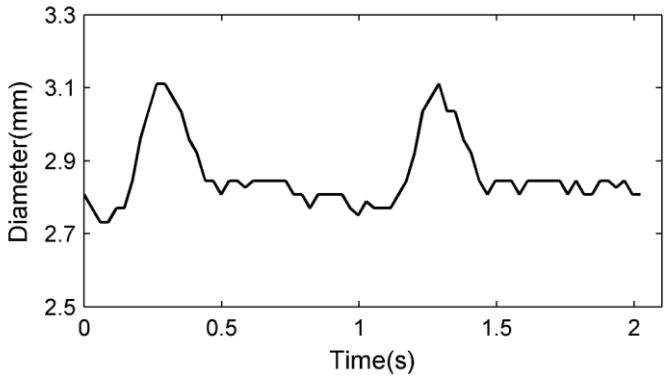

Fig. 6. The pulsatile diameter over two cardiac cycles measured by distance-intensity method

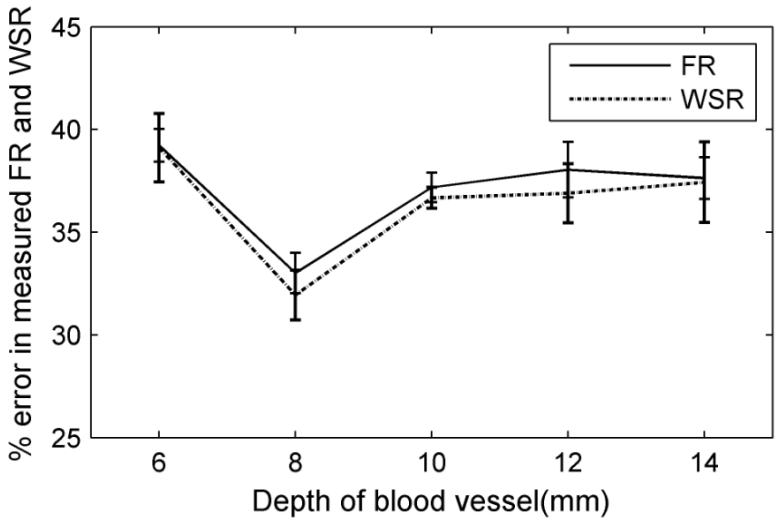

Fig. 7. The % error (mean ± SD) in measured flow rate and wall shear rate at different vessel depths

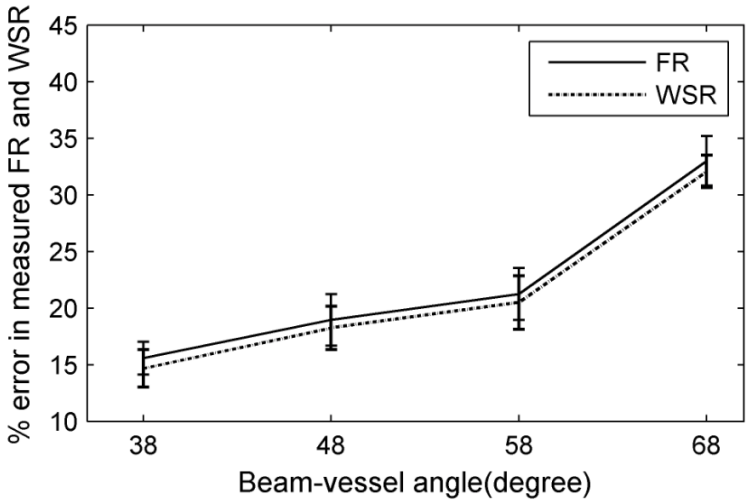

Fig. 8. The % error (mean ± SD) in measured flow rate and wall shear rate at different beam-vessel angles

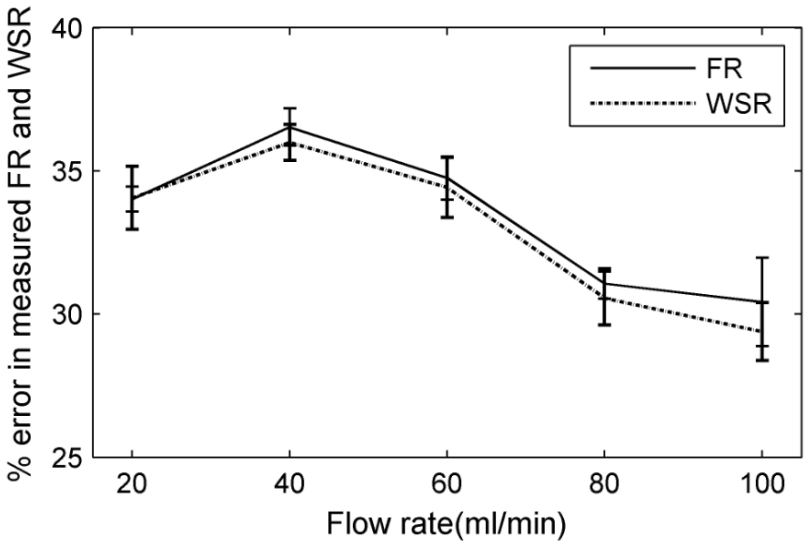

Fig. 9. The % error (mean ± SD) in measured flow rate and wall shear rate at different flow rates

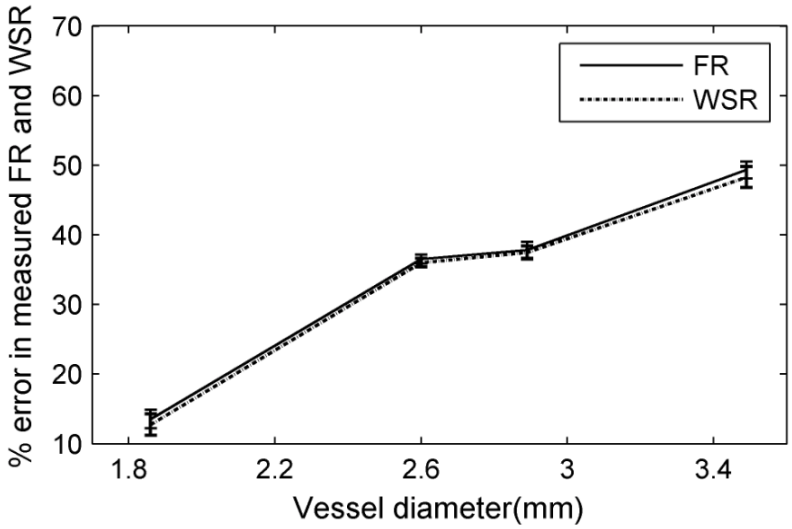

Fig. 10. The % error (mean ± SD) in measured flow rate and wall shear rate at different vessel diameters

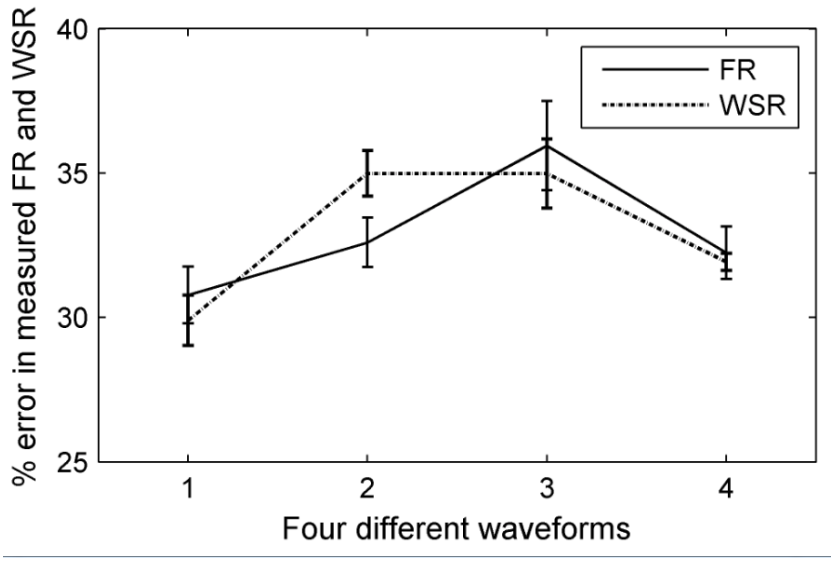

Fig. 11. The % error (mean ± SD) in measured flow rate and wall shear rate at different flow waveforms

Tables

Table 1. The details of these five variables used in the flow phantoms

variables	1	2	3	4	5
Depth(mm)	6	8	10	12	14
Angle(degree)	38°	48°	58°	68°	----
Diameter(mm)	1.86	2.6	2.89	3.49	----
Flow rate(ml min^{-1})	20	40	60	80	100
Waveform	Waveform 1	Waveform 2	Waveform 3	Waveform 4	----

Table 2. The diameters of blood vessels in phantoms under still condition and different flow rates

Flow rate	Phantom1 Diameter(mm) mean ± SD	Phatnom2 Diameter(mm) mean ± SD	Phantom3 Diameter(mm) mean ± SD	Phantom4 Diameter(mm) mean ± SD
0 ml min^{-1}	1.86±0.02	2.60±0.03	2.89±0.03	3.49±0.04
20 ml min^{-1}		2.72±0.03		
40 ml min^{-1}	1.99±0.04	2.89±0.03	3.00±0.03	3.70±0.02
60 ml min^{-1}		3.06±0.03		
80 ml min^{-1}		3.17±0.05		
100 ml min^{-1}		3.25±0.04		